THE EFFECT OF TIMING AND OXIDATION ON EMISSIONS FROM BIODIESEL–FUELED ENGINES

A. Monyem, J. H. Van Gerpen, M. Canakci

ABSTRACT. *The alkyl monoesters of fatty acids derived from vegetable oils or animal fats, known as biodiesel, are attracting considerable interest as an alternative fuel for diesel engines. Biodiesel–fueled engines produce less carbon monoxide, unburned hydrocarbons, and particulate emissions than diesel–fueled engines. However, biodiesel has different chemical and physical properties than diesel fuel, including a larger bulk modulus and a higher cetane number. Some of these properties can be affected by oxidation of the fuel during storage. These changes can affect the timing of the combustion process and potentially cause increases in emissions of oxides of nitrogen.*

The objective of this study was to evaluate the effect of injection and combustion timing on biodiesel combustion and exhaust emissions. A John Deere diesel engine was fueled with two different biodiesel fuels, one of which had been deliberately oxidized, and with their 20% blends with No. 2 diesel fuel. The engine was operated at three different timings and two loads at a single engine speed of 1400 rpm.

The engine performance of the biodiesel was similar to that of No. 2 diesel fuel with nearly the same thermal efficiency. The range of injection timings studied produced changes of 50% and 34% in the CO and HC emissions, respectively. A reduction in NO_x emissions of 35% to 43% was observed for a 3° retarded injection timing compared with a 3° advanced injection timing. A common linear relationship was found between the start of injection and the NO_x emissions for all the fuels studied. When compared at the same start of combustion, the neat biodiesel produced lower NO_x emissions than the No. 2 diesel fuel.

Keywords. *Biodiesel, Diesel, Emissions, Engines, Fuel, Soybean oil.*

Diesel engines are widely used as power sources for medium– and heavy–duty applications because of their lower fuel consumption and lower emissions of carbon monoxide (CO) and unburned hydrocarbons (HC) compared with gasoline engines. For many years, the ready availability of inexpensive middle–distillate petroleum fuels provided little incentive for experimenting with alternative, renewable fuels for diesel engines. However, since the oil crisis of the 1970s, research interest has expanded in the area of alternative fuels. In recent years, the potential environmental benefits of alternative fuels have also attracted attention.

Many researchers have concluded that vegetable oils hold promise as alternative fuels for diesel engines (Goering et al., 1982; Sims, 1985). Using raw vegetable oils in diesel engines can cause numerous engine–related problems. The increased viscosity and low volatility of vegetable oils lead to severe engine deposits, injector coking, and piston ring sticking (Perkins et al., 1991; Pestes and Stanislao, 1984). However, these effects can be reduced or eliminated through transesterification of the vegetable oil to form a monoester, generally known as "biodiesel" (Perkins et al., 1991; Zhang et al., 1988). This process decreases the viscosity, maintains the heating value, and may actually increase the cetane number. It has also been found that biodiesel can provide a substantial reduction in HC, CO, and particulate emissions, although often at the cost of an increase in NO_x emissions (Chang et al., 1996; Last et al., 1995; Schumacher et al., 1993).

A number of diesel emissions studies have been conducted with biodiesel and blends of biodiesel, but few have dealt with injection timing effects, and none have included the effects of fuel oxidation on engine emissions and biodiesel combustion. The objective of this study was to evaluate the effect of injection timing and fuel oxidation on biodiesel combustion and exhaust emissions.

EQUIPMENT AND PROCEDURES

ENGINE TEST SETUP AND EXHAUST SAMPLING PROCEDURE

A John Deere 4276T four–cylinder, four–stroke, turbocharged DI diesel engine with a bore of 106.5 mm, a stroke of 127.0 mm, a displacement of 4.53 L, and a compression ratio of 16.8:1 was connected to a 112 kW (150 hp) General Electric model TLC2544 DC electric dynamometer. A portion of the exhaust gas was passed through a 190° C heated sampling line and filter to the emission analyzers. A Beckman model 402 heated flame ionization detector hydrocarbon analyzer and a Beckman model 7003 polarigraphic oxygen monitor were used to measure the concentrations of HC and oxygen (O_2) in the exhaust gas. Two Beckman model 864 infrared analyzers measured the concentrations of CO and carbon dioxide (CO_2) in the engine exhaust. A Thermo Environmental Instruments Inc. Model 42H chemiluminescent NO–NO_2–NO_x analyzer and a Thermo Environmental Instruments Inc. Model 350 chemiluminescent NO–NO_2–NO_x analyzer were used to gather duplicate measurements of the concentration of NO_x.

Article was submitted for review in January 2000; approved for publication by the Power & Machinery Division of ASAE in August 2000.

The authors are **Abdul Monyem,** Design Engineer, Caterpillar, Inc., Mossville, Illinois; **Jon H. Van Gerpen,** ***ASAE Member Engineer,*** Professor, and **Mustafa Canakci,** Research Assistant, Department of Mechanical Engineering, Iowa State University, Ames, Iowa. **Corresponding author:** Jon H. Van Gerpen, Dept. of Mechanical Engineering, Iowa State University, Ames, IA 50011; phone: 515–294–5563; fax: 515–294–3261; e–mail: jvg@iastate.edu.

A Bosch smoke meter was used to measure the smoke level. The gaseous emissions were expressed on a brake–specific basis and each data point was the average of three independent measurements. An electronic scale and a stopwatch were used to measure the fuel flow rate.

A Kistler model 6061B pressure transducer was installed in the No. 1 cylinder, and a Kistler model 6230M1 pressure transducer was installed in the No. 1 cylinder fuel injection line. The cylinder and injection pressure data were collected using the Labview computer program with a 486 computer and a National Instruments Model ATMIO–16 data acquisition system. The data acquisition system collected the pressure data every 0.25 degrees of crankshaft rotation, and 50 cycles were averaged.

Fuel Preparation

The biodiesel was soybean oil–based and was purchased from NOPEC Corporation (Lakeland, Florida). Its chemical properties are given in table 1. The oxidized biodiesel was prepared by heating 83 L of biodiesel to 60° C in a 208–L container while bubbling oxygen (99.6% purity) through the fuel at the rate of 0.4 m^3/h. The fuel's peroxide value, as measured by the American Oil Chemist's Society method Cd 8–53 (AOCS, 1993), was used as the indicator of the extent of oxidation. It was desired to elevate the fuel peroxide value quickly without allowing the fuel viscosity to increase excessively. The biodiesel was oxidized from a starting peroxide value of 30–40 meq O_2/kg to 340 meq O_2/kg in 6–8 h. The oxidized and unoxidized biodiesels, their 20% blends (by weight), and the base fuel (No. 2 diesel) were tested in the engine at two different loads (100% and 20%) and at three injection timings (3° advanced, standard, and 3° retarded). The tests were performed at steady–state conditions at a single engine speed of 1400 rpm. The full–load (100%) torque was 258 N–m and the 20% load torque was 52 N–m.

Table 1. Fuel analysis.

	No. 2 Diesel	Biodiesel	Oxidized Biodiesel
Molecular wt.	198	291.6	N.A.
Carbon (%)	86.23	76.14	76.06
Hydrogen (%)	13.14	11.75	11.51
Sulfur (%)	0.034	<0.005	0.010
CetaneNumber (D613)	47.4	51.1	72.7
Heat of Combustion			
Gross (kJ/kg)	45504	39766	38896
Net (kJ/kg)	42716	37273	36454
Hydrocarbon types			
Saturates (%)	64.1	N.A.	N.A.
Olefins (%)	4.9	N.A.	N.A.
Aromatics (%)	31.0	0	0
Viscosity (cS)		4.63	
Free glycerin		0.004	
Monoglycerides (%)		0.352	
Diglycerides (%)		0.132	
Triglycerides (%)		0.152	
Total glycerin (%)		0.131	
Biodiesel Fatty Acid Composition			
Palmitic (16:0) (%)		10.76	
Stearic (18:0) (%)		4.37	
Oleic (18:1) (%)		24.13	
Linoleic (18:2) (%)		51.83	
Linolenic (18:3) (%)		6.81	

N.A. = Not available

Data Analysis

Statistical Analysis

In addition to the engine operating variables of load, timing, and fuel type, the oxidized fuel batch number and the age of the fuel were included as test variables to determine whether they had any effect on engine emissions. A simple factorial design was not considered to be appropriate for this test because all of the variables could not be tested independently on any given day. Due to the time required to set the fuel injection timing, only a single value could be tested each day. This limitation mandated the use of a split–plot experimental design.

The split–plot statistical design consists of two stages. The first stage is related to the whole plot, and the second stage is related to a subplot. In this design, a single test day is considered a whole plot, and each of the ten test conditions within a day is considered a sub–plot. This split–plot design is shown in tables 2 and 3. The whole plot is a 3×3 Latin square, and within each whole day plot is a 2×5 factorial experiment. A 3×3 Latin square contains 3 rows and 3 columns (table 2). The three treatments (injection timings) are randomly assigned to experimental units within the rows and columns so that each treatment appears in every row and in every column. The 2×5 factorial experiment identifies the ten randomly chosen combinations of load and fuel type to be run each day (table 3). An SAS program was used to analyze the collected data. More extensive explanation of these topics is provided in Ott (1993) and Neter et al. (1996).

Calculation of Ignition Delay

Ignition delay was defined as the time between the start of fuel injection and the start of combustion. The start of injection is usually taken as the time when the injector needle lifts off its seat. Because a needle lift detector was not available, the start of injection was defined to be the point when the injection line pressure reached 207 bar, the nozzle–opening–pressure for the injector. The start of combustion was defined in terms of the change in slope of the heat–release rate that occurs at ignition. The heat release rate was calculated using a technique similar to that described by Krieger and Borman (1966).

Table 2. Whole plot (3×3 Latin square).

	Age		
Batch	1	2	3
1	Standard (Day 1)	3° Advanced (Day 2)	3° Retarded (Day 3)
2	3° Retarded (Day 4)	Standard (Day 5)	3° Advanced (Day 6)
3	3° Advanced (Day 7)	3° Retarded (Day 8)	Standard (Day9)

Table 3. Randomly assigned subplot within each whole plot (2×5 factorial experiment).

	Fuel				
Load	100% HPVB	100% LPVB	20% HPVB	20% LPVB	No. 2 Diesel
100%	10th	5th	9th	3rd	1st
20%	4th	8th	7th	6th	2nd

Results And Discussion

The Effect of Timing on Diesel Engine Exhaust Emissions

Figure 1 shows the percent change in emissions compared to the base diesel fuel for the 3° advanced, standard, and 3° retarded injection timings at the full–load engine condition. In these figures, all emissions comparisons are shown relative to the No. 2 diesel fuel at the same timing. A reduction in the CO, HC, and smoke number (SN) were observed for all fuel blends at all injection timings compared with No. 2 diesel fuel. The maximum reduction in these emissions was found for the oxidized biodiesel. However, the NO_X emissions increased for all fuel blends at all injection timings. The smoke number, CO, and HC were decreased by 8% to 63%, 2% to 29%, and 3% to 60%, respectively, while the NO_X emissions increased by 0.5% to 18%. Regardless of the injection timing, the oxidized neat biodiesel reduced the CO and HC emissions by 4% to 15% and 9% to 16%, respectively, compared with unoxidized neat biodiesel. The emissions of CO_2 showed mixed results with the percentage changes being very small.

Figure 2 shows the percent change in emissions at the light–load engine condition for the three timings. At light load, the smoke level was near the detection threshold of the smoke meter, so these measurements were not shown on the figure. As was observed at high load, there was a reduction in CO and HC emissions regardless of the injection timing and fuel. These CO and HC reductions were in the range of 10% to 56% and 6% to 66%, respectively. The oxidized neat biodiesel reduced the CO and HC emissions more than the unoxidized biodiesel by 16% to 25% and 20% to 29%, respectively, over the range of injection timings studied. An increase in NO_X emissions was found for the 3° advanced injection timing, and a reduction in NO_X emissions was found for the 3° retarded injection timing for all fuel blends.

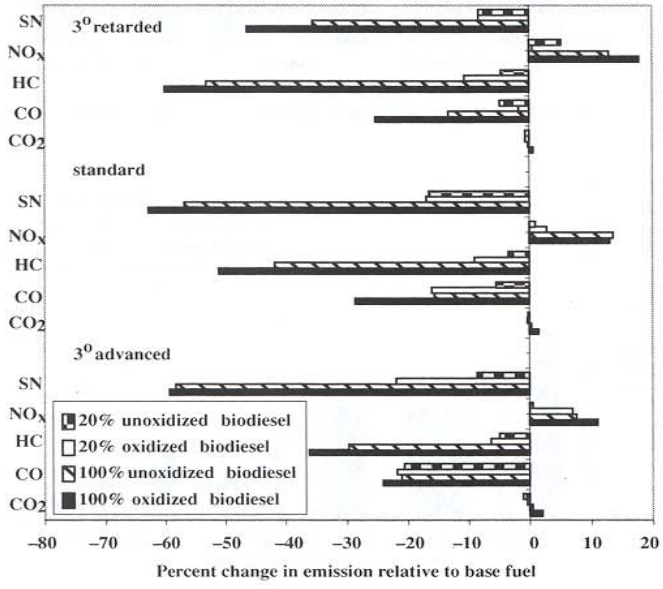

Figure 1. Percent change in emissions relative to base fuel at full–load engine condition.

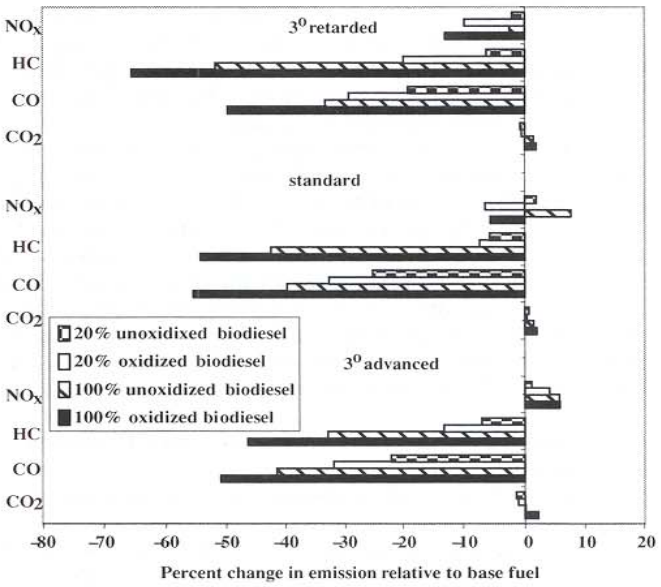

Figure 2. Percent change in emissions relative to base fuel at light–load engine condition.

Combustion Characteristics

Comparison of the Start of Fuel Injection

Three different fuel injection pump timing settings were used for this study: 3° retarded, standard, and 3° advanced. The degrees of timing change refer to crankshaft degrees. The actual start of fuel injection is affected by the pump setting, but it can also be influenced by changes in fuel properties such as the viscosity, the bulk modulus, and the speed of sound (Obert, 1973). The start of fuel injection is important because fuel injected early produces higher flame temperatures and may contribute to higher NO_X emissions.

The effect of changes in fuel injection timing on the start of combustion is complicated by the effect of the different fuel cetane numbers. The cetane number is an indicator of the time delay between when the fuel is injected and when it starts to burn.

The injection line pressure with standard timing and at the full–load engine condition for all five tested fuels is shown in figure 3. Even though the fuel injection pump timing was

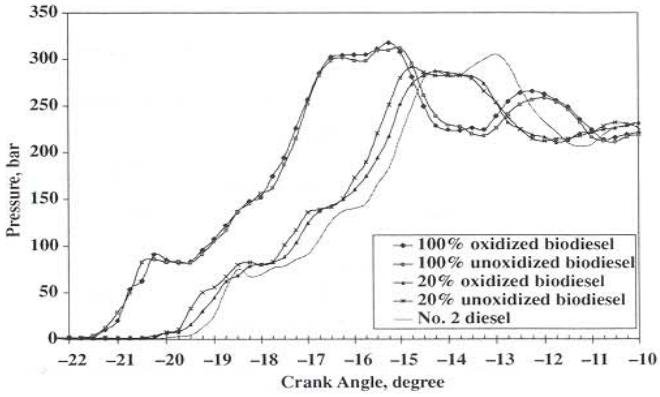

Figure 3. Injection line pressure with standard timing and full–load engine condition.

not altered as the fuels were changed, it is clear that the neat biodiesel fuels had earlier actual injection timings. The oxidized and unoxidized biodiesel fuels both injected about 2.3° earlier than the No. 2 diesel fuel. The 20% blends were 0.25–0.75° earlier than the No. 2 diesel fuel.

Figure 4 shows the start of fuel injection into the cylinder for all three injection timings (3° advanced, standard, and 3° retarded) at the full–load engine condition. Each bar on these figures is the average of three measurements collected on separate days. The error bands show the extent of the maximum and minimum values of the three measurements. The injection timings were set every day and were confirmed using the data acquisition system. Figure 4 shows a consistent tendency for earlier injection timing by the neat biodiesel fuels due to differences in their physical properties.

Comparison of the Start of Combustion Times and Fuel Burning Rates

In this study, start of combustion was defined as the time when the heat–release rate calculated from the cylinder pressure data started to rise rapidly. Figure 5 shows the heat–release profiles with standard timing for all five fuels. The oxidized biodiesel showed the most advanced start of combustion. This was expected based on its high cetane number, as reported in table 1. The next most advanced start of combustion was found for the unoxidized biodiesel. The 20% blends and No. 2 diesel fuel show almost no difference in the start of combustion. Compared to the base fuel, the oxidized biodiesel had about 3.3° earlier start of combustion with standard timing, while the unoxidized biodiesel had only 2.3° earlier start of combustion.

Figures 6 and 7 show the measured start of combustion with the three different timings at the full–load (fig.6) and light–load (fig 7) engine conditions. The start of combustion was earlier for the oxidized biodiesel compared to No. 2 diesel fuel. The unoxidized biodiesel also advanced the start of combustion, but the other fuels (the 20% blends and No. 2 diesel) showed somewhat mixed results at the full–load engine condition. At the light–load engine condition, the start of combustion was more retarded than at the full–load engine condition. The oxidized biodiesel at this load showed the most advanced start of combustion, while the No. 2 diesel fuel showed the most retarded. These differences in the start of combustion are the result of two factors: 1) Biodiesel should have a shorter ignition delay, as indicated by its higher cetane number, and 2) Biodiesel's different physical properties, such as higher bulk modulus, viscosity, and speed of sound, can also cause an earlier injection event (Gouw and Vlugter, 1964; Tat and Van Gerpen, 1999; Tat et al., 2000).

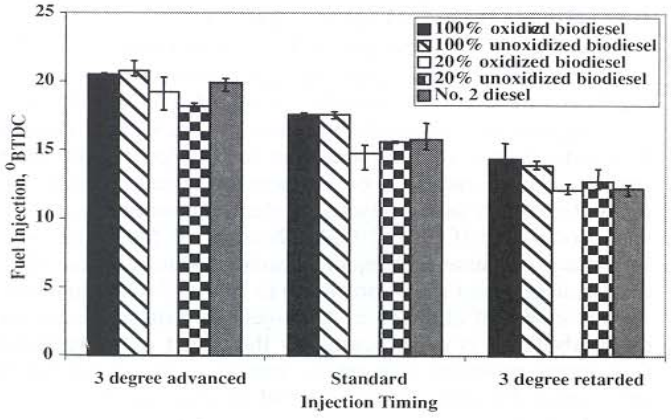

Figure 4. Fuel injection at full–load engine condition.

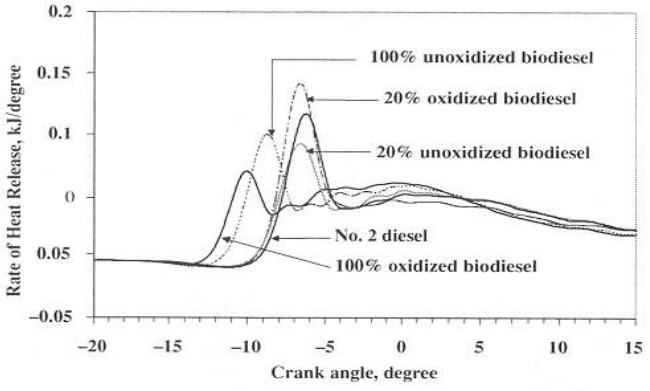

Figure 5. Heat–release profiles with timing at full–load engine condition.

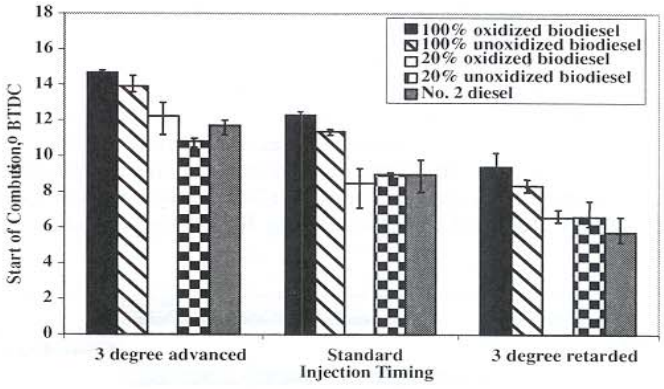

Figure 6. Start of combustion at full–load engine condition.

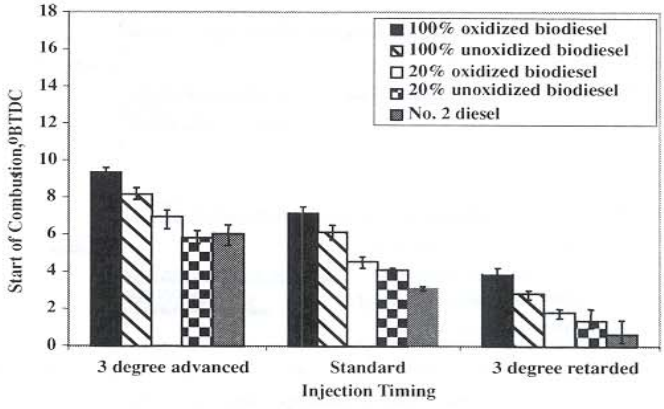

Figure 7. Start of combustion at light–load engine condition.

Discussion of Observed Trends

Effect of Ignition Delay on HC Emissions

Most HC emissions in diesel engines originate in regions where excessive dilution with air prevents combustion because the fuel–air mixture is past the lean combustion limit. The magnitude of the unburned HC from these over–lean regions is related to the amount of fuel injected during the ignition delay period, before combustion starts. Figure 8 confirms this correlation between HC emissions and ignition delay for the light–load operating condition, where the HC emissions are highest. This figure includes data for all five fuels and all three injection timings. The data show the expected trend: the HC emissions decrease as the ignition delay gets shorter. The HC emissions for all fuels and for all injection timings appear to fall on one line. This correlation was unexpected given the large differences in volatility and oxygen content of these fuels.

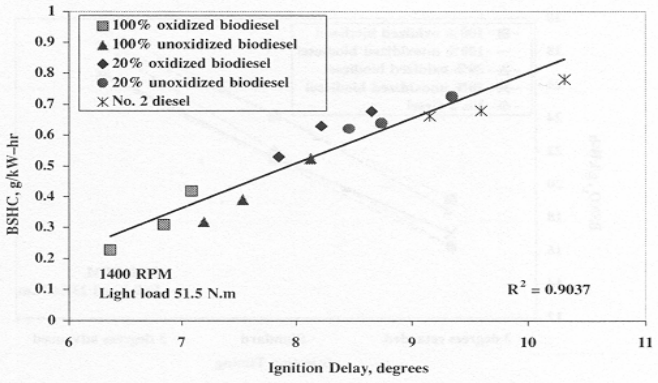

Figure 8. Brake–specific HC emissions as a function of ignition delay at light–load engine condition.

Effect of the Start of Fuel Injection and the Start of Combustion on NO_X Emissions

Generally, NO_X emissions form in the high–temperature regions of the combustion chamber, where the air/fuel ratio is slightly below stoichiometric. Springer and Patterson (1972) noted that increases in the local temperature and the oxygen concentration within the diesel spray envelope increase the NO_X emissions. One theory that has been proposed for the increased NO_X observed with biodiesel is that the oxygen contained in the fuel makes more oxygen available in the reaction zone during combustion, and this causes the NO_X emissions to rise (Rickeard and Thompson, 1993).

To investigate the effect of biodiesel combustion on the flame temperature, calculations were performed to determine the adiabatic flame temperature for biodiesel combustion compared with diesel fuel combustion. Figure 9 shows the stoichiometric adiabatic flame temperature for biodiesel and for No. 2 diesel fuel. The calculations show that for both constant–volume combustion and constant–pressure combustion, the flame temperature for biodiesel is slightly below that for diesel fuel. This indicates that flame temperature changes alone cannot adequately explain the higher levels of NO_X observed with biodiesel.

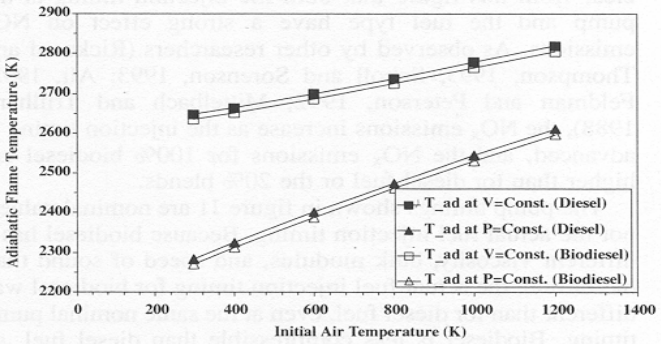

Figure 9. Stoichiometric adiabatic flame temperature for biodiesel and diesel fuel.

The emissions comparisons presented in this article were conducted with the engine adjusted to produce the same torque level with each fuel. This means that the fuel flow rate of the biodiesel was increased compared with diesel fuel to compensate for biodiesel's lower energy content. Because most engines are limited by the volume of fuel that can be injected, many researchers have evaluated biodiesel in unmodified engines, where biodiesel's lower energy content causes lower maximum torque. Figure 10 shows a comparison of the adiabatic flame temperature for diesel fuel at an equivalence ratio of 0.6, a typical full–load value, with the flame temperature for biodiesel at 0.5434, a value that corresponds to the same volume of fuel delivery. In this case, the flame temperatures are substantially lower for biodiesel. These data further indicate that flame temperature is probably not the reason for the higher NO_X levels observed with biodiesel.

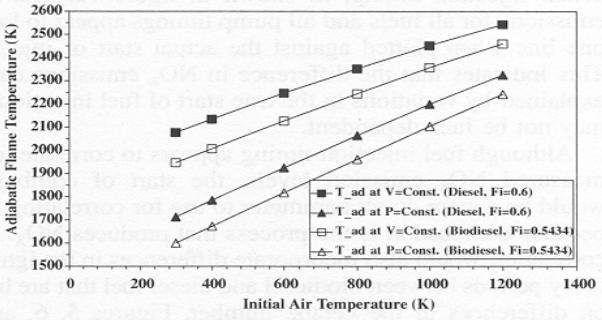

Figure 10. Adiabatic flame temperature for equal fuel volumes of biodiesel and diesel fuel.

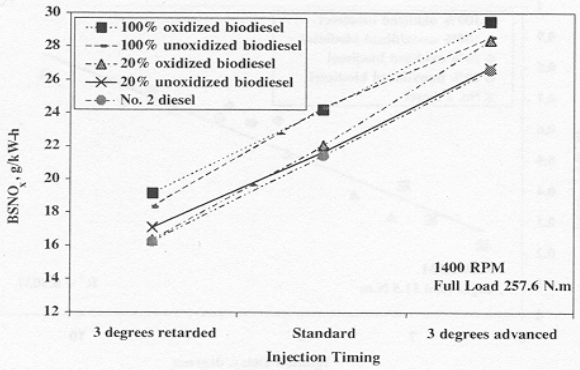

Figure 11. Brake–specific NO_x emissions vs. pump timing at full–load engine condition.

The NO_x emissions with the three different pump timings at the full–load engine condition are shown in figure 11. It is clear from this figure that both the injection timing at the pump and the fuel type have a strong effect on NO_x emissions. As observed by other researchers (Rickeard and Thompson, 1993; Scholl and Sorenson, 1993; Ali, 1995; Feldman and Peterson, 1992; Mittelbach and Trillhart, 1988), the NO_x emissions increase as the injection timing is advanced, and the NO_x emissions for 100% biodiesel are higher than for diesel fuel or the 20% blends.

The pump timings shown in figure 11 are nominal values, not the actual fuel injection timing. Because biodiesel has a different viscosity, bulk modulus, and speed of sound than diesel fuel, the actual fuel injection timing for biodiesel was different than for diesel fuel, even at the same nominal pump timing. Biodiesel is less compressible than diesel fuel, so pressure can develop faster—and pressure waves can propagate faster—in biodiesel than in diesel fuel. This is the reason for the advanced injection timing of biodiesel noted earlier. This advanced injection may contribute to the additional NO_x emissions for biodiesel. To investigate this effect, the full–load NO_x emissions were plotted against the actual injection timing, as shown in figure 12. The NO_x emissions for all fuels and all pump timings appear to fall on one line when plotted against the actual start of injection. This indicates that the difference in NO_x emissions can be explained by variations in the true start of fuel injection and may not be fuel–dependent.

Although fuel injection timing appears to correlate to the measured NO_x emission levels, the start of combustion would be a more direct parameter to use for correlating NO_x because combustion is the process that produces NO_x. This correlation would also incorporate differences in the ignition delay periods between biodiesel and diesel fuel that are based on differences in the cetane number. Figures 5, 6, and 7 showed that the start of combustion was more advanced for biodiesel than for diesel fuel due to its higher cetane number, causing a shorter ignition delay and conforming to biodiesel's earlier actual injection timing. However, the shorter ignition delay will also cause less premixed combustion, which has been identified as a source of NO_x production in naturally aspirated and lightly turbocharged engines (Chan and Borman, 1982).

When the NO_x data are plotted against the start of combustion, as shown in figure 13, differences between the fuels emerge again. These plots indicate that for the same start of combustion timing, the 100% biodiesel fuels actually produced less NO_x than diesel fuel. This result is probably attributable to the lower amount of premixed combustion with biodiesel due to its higher cetane number. This result may be engine–specific because Donahue, et al. (1994) have noted that the correlation between premixed combustion and NO_x decreases for highly turbocharged engines.

Tradeoff between NO_x Emissions and Smoke Emissions

Figure 14 shows the tradeoff relationships between the NO_x emissions and the smoke number as the actual fuel injection timing was varied. The figure indicates that, for this diesel engine, oxidized neat biodiesel shows a better tradeoff than No. 2 diesel fuel. The tradeoff curves for neat unoxidized biodiesel and the 20% blends are between oxidized neat biodiesel and No. 2 diesel fuel.

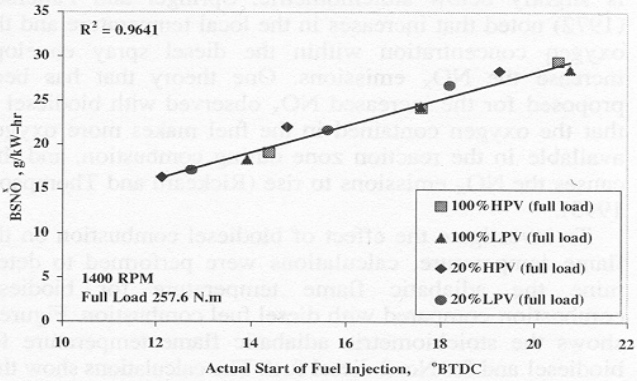

Figure 12. Brake–specific NO_x emissions as a function of start of fuel injection.

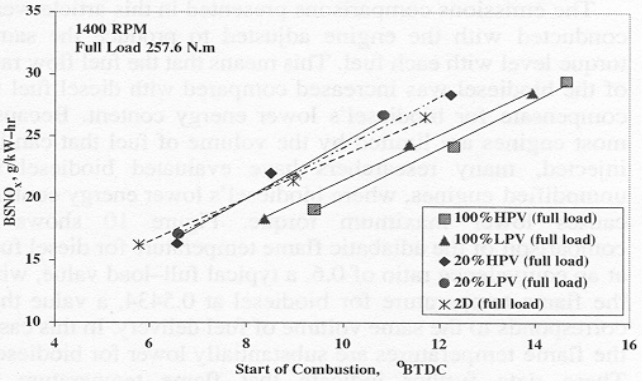

Figure 13. Brake–specific NOx emissions as a function of start of combustion at full–load engine condition.

CONCLUSIONS

The objectives of this study were to understand the effect of timing and fuel oxidation on biodiesel exhaust emissions and combustion. Based on the experimental results and the above discussion, the following conclusions can be drawn:

1. Biodiesel, particularly if oxidized, has lower CO and HC emissions than No. 2 diesel fuel. The retarded injection timing produced 50% less CO emissions and 34% less HC emissions than the advanced injection timing for neat oxidized biodiesel.
2. Retarded injection timing significantly reduced NO_X emissions. The 3° retarded injection timing gave a 20.9% reduction in NO_X emissions for neat oxidized biodiesel at the full–load engine condition compared with standard injection timing.
3. Injection timing had a significant effect on smoke number. The advanced injection timing gave a lower smoke number than the retarded injection timing. The Bosch Smoke Number for the oxidized biodiesel increased from 0.4 (for the 3° advanced timing) to 1.0 (for the 3° retarded timing). The Bosch Smoke Number for No. 2 diesel fuel increased from 1.0 to 1.9 over this range of timings.
4. The actual fuel injection timing was advanced for neat biodiesel compared with diesel fuel at the same injection pump settings due to differences in the physical properties of the fuels. Compared with diesel fuel, the fuel injection timing for the two neat biodiesels was about 2.3° advanced.
5. The oxidized and unoxidized biodiesels experienced shorter ignition delays than diesel fuel and had less premixed burning. The neat oxidized biodiesel had a 0.9° shorter ignition delay than the neat unoxidized biodiesel at standard timing. Retarded injection timing reduced the ignition delay for all fuels.
6. Shorter ignition delay reduced HC emissions. The ignition delay was linearly correlated to HC emissions with no effect of fuel type.
7. A common linear relationship was found between NO_X emissions and the start of fuel injection that showed no effect of fuel type. However, when NO_X was plotted against the start of combustion, there were differences between the fuels. At the same start of combustion, the neat biodiesel fuels were found to produce less NO_X than the No. 2 diesel fuel.
8. The relationship between NO_X emissions and smoke number for biodiesel showed that both oxidized and unoxidized biodiesels provide a superior tradeoff compared with No. 2 diesel fuel.

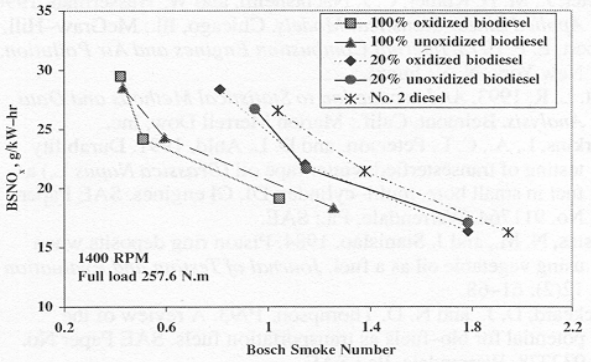

Figure 14. Brake–specific NOx vs. smoke number at full–load engine condition.

REFERENCES

Ali, Y. 1995. Beef tallow as a biodiesel fuel. Ph.D. diss. Univeristy of Nebraska, Lincoln.

AOCS. 1993. 4th Ed. *Official Methods and Recommended Practices of the American Oil Chemists' Society*. Champaign, Ill.: AOCS Press.

Chan, T. T., and G. L. Borman. 1982. An experimental study of swirl and EGR effects on diesel combustion by use of the dumping method. SAE Paper No. 820359. Warrendale, Pa.: SAE.

Chang, D. Y. Z., J. H. Van Gerpen, I. Lee, L. A. Johnson, E. G. Hammond, and S. J. Marley. 1996. Fuel properties and emissions of soybean oil esters as diesel fuel. *JAOCS* 73(11): 1549–1555.

Donahue, R. J., G. L. Borman, and G. R. Bower. 1994. Cylinder–averaged histories of nitrogen oxide in a D.I. diesel with simulated turbocharging. SAE Paper No. 942046. Warrendale, Pa.: SAE.

Feldman, M. E., and C. L. Peterson. 1992. Fuel injection timing and pressure optimization on a DI diesel engine for operation on biodiesel. *Liquid Fuels From Renewable Resources: Proceedings Of An Alternative Energy Conference,* 14–15 December. St. Joseph, Mich.: ASAE.

Goering, C. E., A. W. Schwab, M. J. Dangherty, E. H. Pryde, and A. J. Heakin. 1982. Fuel properties of eleven vegetable oils. *Trans. ASAE* 25(6): 1472–1477, 1483.

Gouw, T. H., and J. C. Vlugter. 1964. Physical properties of fatty acid methyl esters, IV. Ultrasonic sound velocity. *JAOCS* 41(8): 524–526.

Krieger, R. B., and G. L. Borman. 1966. The computation of applied heat release for internal combustion engines. ASME Paper No. 66–WA/DGP–4. New York, N. Y.: ASME.

Last, J. R., M. K. Kruger, and M. Durnholz. 1995. Emissions and performance characteristics of a 4–stroke, direct injection diesel engine fueled with blends of biodiesel and low sulfur diesel fuel. SAE Paper No. 950054. Warrendale, Pa.: SAE.

Mittelbach, M., and P. Trillhart. 1988. Diesel fuel derived from vegetable oils, III. Emission tests using methyl esters of used frying oil. *JAOCS* 65(7): 1185–1187.

Neter, J., M. H. Kutner, C. J. Nachtsheim, and W. Wasserman. 1996. *Applied Linear Statistical Models*. Chicago, Ill.: McGraw–Hill.

Obert, E. F. 1973. *Internal Combustion Engines and Air Pollution*. New York, N. Y.: Intext.

Ott, L. R. 1993. *An Introduction to Statistical Methods and Data Analysis*. Belmont, Calif.: Marion Merrell Dow, Inc.

Perkins, L. A., C. L. Peterson, and D. L. Auld. 1991. Durability testing of transesterfied winter rape oil (*Brassica Napus* L.) as fuel in small bore, multi–cylinder, DI, CI engines. SAE Paper No. 911764. Warrendale, Pa.: SAE.

Pestes, N. M., and J. Stanislao. 1984. Piston ring deposits when using vegetable oil as a fuel. *Journal of Testing and Evaluation* 12(2): 61–68.

Rickeard, D. J., and N. D. Thompson. 1993. A review of the potential for bio–fuels as transportation fuels. SAE Paper No. 932778. Warrendale, Pa.: SAE.

Scholl, K. W., and S. C. Sorenson. 1993. Combustion of soybean oil methyl ester in a direct injection diesel engine. SAE Paper No. 930934. Warrendale, Pa.: SAE.

Schumacher, L. G., S. C. Borgelt, W. G. Hires, C. Spurling, J. K. Humphrey, and J. Fink. 1993. Fueling diesel engines with esterified soybean oil. ASAE Paper No. MC93–101. Presented at the 1993 Mid–Central Conference of the ASAE. St. Joseph, Mich.: ASAE.

Sims, R. E. H. 1985. Tallow esters as an alternative diesel fuel. *Trans. of the ASAE* 28(3): 716–721.

Springer, G. S., and D. J. Patterson. 1972. *Engine Emissions: Pollutant Formation and Measurement*. New York, N. Y.: Plenum Press.

Tat, M. E., and J. H. Van Gerpen. 1999. The kinematic viscosity of biodiesel and its blends with diesel fuel. *JAOCS* 76(12): 1511–1513.

Tat, M. E., J. H. Van Gerpen, S. Soylu, M. Canakci, A. Monyem, and S. Wormley. 2000. The speed of sound and isentropic bulk modulus of biodiesel at 21°C from atmospheric pressure to 35 MPa. *JAOCS* 77(3): 285–289.

Zhang, Q., M. Feldman, and C. L. Peterson. 1988. Diesel engine durability when fueled with methyl ester of winter rapeseed oil. ASAE Paper No. 88–1562. St. Joseph, Mich.: ASAE.